






Article

In Silico Design of Novel Piperazine-Based mTORC1 Inhibitors Through DFT, QSAR and ADME Investigations

El Mehdi Karim ¹, Oussama Abchir ¹, Hassan Nour ¹, Ossama Daoui ², Souad El Khattabi ², Farhan Siddique ³, M'Hammed El Kouali ¹, Mohammed Talbi ¹, Abdelkbir Errougui ¹ and Samir Chtita ^{1,*}

- ¹ Laboratory of Analytical and Molecular Chemistry, Faculty of Sciences Ben M'Sik, Hassan II University of Casablanca, Casablanca P.O. Box 7955, Morocco; 2013karim.mehdi@gmail.com (E.M.K.); oussamaabchir12@gmail.com (O.A.); hassannour737@gmail.com (H.N.); m.elkouali@gmail.com (M.E.K.); talbi.uh2c@gmail.com (M.T.); a_errougui@yahoo.fr (A.E.)
- ² Laboratory of Engineering, Systems and Applications, National School of Applied Sciences, Sidi Mohamed Ben Abdellah-Fez University, Fez P.O. Box 72, Morocco; daoui.ossama@gmail.com (O.D.); souad.elkhattabi@usmba.ac.ma (S.E.K.)
- ³ Departement of Farmaceutical Chemistry, Faculty of Pharmacy, Bahahuddian Zakariya University, Multan 60800, Pakistan; drfarhansiddique@bzu.edu.pk
- * Correspondence: samirchtita@gmail.com

Abstract: Mammalian target of rapamycin complex 1 (mTORC1) is an important and promising alternative biological target for the treatment of different types of cancer including breast, lung and renal cell carcinoma. This study contributed to the development of mathematical models highlighting the quantitative structure-activity relationship of a series of piperazine derivatives reported as mTORC1 inhibitors. Various molecular descriptors were calculated using Gaussian 09, Chemsketch, and ChemOffice software. The density functional theory (DFT) method at the level B3LYP/6-31G+(d, p) was applied to determine the structural, electronic and energetic parameters associated with the studied molecules. The predictive ability of the built models, which is obtained by two methods (MLR and MNLR), showed that the built models are statistically significant. The QSAR modeling results revealed that the six molecular descriptors of lowest unoccupied molecular orbital energy (ELUMO), electrophilicity index (ω), molar refractivity (MR), aqueous solubility (Log S), topological polar surface area (PSA), and refractive index (n) significantly correlated to the biological inhibitory activity of piperazine derivatives. Using QSAR models and in silico pharmacokinetic profiles predictions, five new candidate compounds are selected as potential inhibitors against cancer.

Keywords: 2D-QSAR; anti-cancer; mTORC1 Inhibitors; piperazine derivatives; DFT; ADME



Citation: Karim, E.M.; Abchir, O.; Nour, H.; Daoui, O.; El Khattabi, S.; Siddique, F.; El Kouali, M.; Talbi, M.; Errougui, A.; Chtita, S. In Silico Design of Novel Piperazine-Based mTORC1 Inhibitors Through DFT, QSAR and ADME Investigations. *Biophysica* **2024**, *4*, 517–529. <https://doi.org/10.3390/biophysica4040034>

Academic Editor: Paulino Gómez-Puertas

Received: 13 September 2024
Revised: 29 September 2024
Accepted: 11 October 2024
Published: 24 October 2024

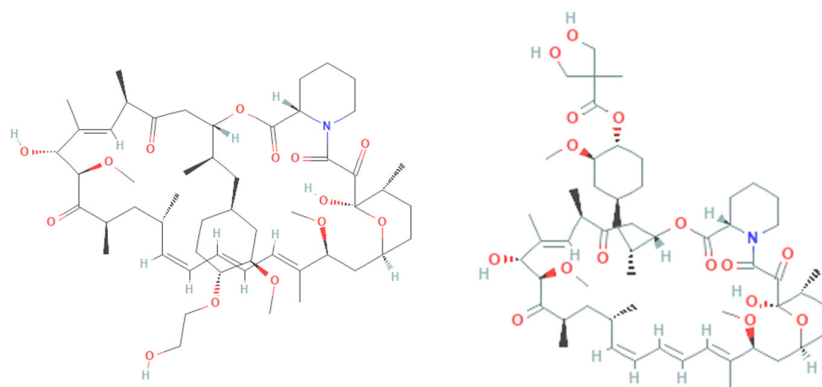


Copyright: © 2024 by the authors. Licensee MDPI, Basel, Switzerland. This article is an open access article distributed under the terms and conditions of the Creative Commons Attribution (CC BY) license (<https://creativecommons.org/licenses/by/4.0/>).

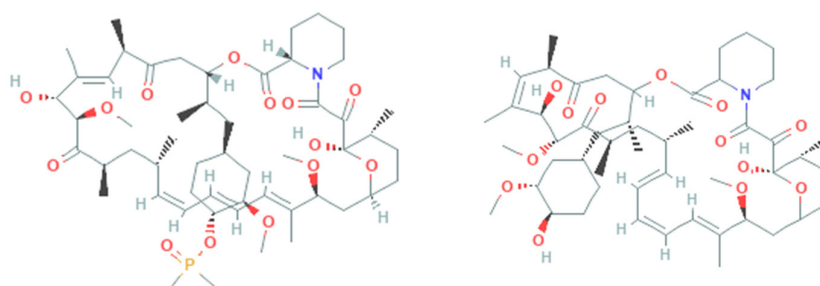
1. Introduction

Breast, lung and renal cell carcinomas are among the most dangerous cancers, with rapid metastasis, progression and high mortality, especially when detected late [1]. Although, many therapies for advanced cancers have recently been established, the disease has not yet been defeated; resistance develops due to cancer heterogeneity, alternative pathways (signalling) and some severe adverse conditions, which limits the potency of new treatments [2]. Although therapeutic alternatives are now available and are more effective than before for patients with advanced cancer, there is still a need to develop new potent drugs that target melanoma, and several techniques are being used, ranging from exploring a better delivery system for existing compounds to evaluating new targets [3,4]. The mTORC1 kinase has been identified as a promising target in cancer therapy, it is inhibited by rapamycin, which disrupts the mTORC1 signaling pathway [5]. A series of rapamycin is optimized and used in the creation of new natural clinical candidates such as Everolimus (RAD001), Temsirolimus (CCI-779) and Ridaforolimus (MK-8669) whose inhibitory activities respectively (8.26, 5.8 and 9.7) (Figure 1) [5], which demonstrated

significant serine/threonine inhibition of mTORC1 kinase in both in vitro and in vivo tests, as well as excellent pharmaceutical properties and strong inhibition of cancer and tumor growth [6]. These larger, natural molecules have been reported as mTORC1 inhibitors, but they have a high molecular weight, greater than 500 Daltons (Lipinski's rule states that a substance must have a molecular weight of less than 500 Daltons to be able to cross the skin barrier), which deviates from Lipinski's rule of 5 [7].



Everolimus Temsirolimus



Ridaforolimus Rapamycin

Figure 1. Structures of currently available natural mTORC1 inhibitors.

QSAR and DFT approaches have recently been exploited with the aim of investigating mTORC1 inhibition for the discovery of new potent molecules to be used in the cure of tumors. Chaube et al. have investigated the binding interactions with the mTORC1 protein, further supported by QSAR studies, highlighting interactions playing a key role in the design of potent mTORC1 inhibitors [8]. Similarly, Kaavin et al. used DFT and molecular docking studies to assess the stability and reactivity of a series of novel transition metal complexes targeting proteins, including mTORC1, which provided an insight into their high protein-binding affinities [9]. Essentially, such computer-aided studies identify key molecular features responsible for enhanced mTORC1 inhibition and help guide drug design.

Piperazine derivatives have recently received great interest in the world of drug discovery due to their antipsychotic, depressant, anxiolytic, antitumor and anticancer abilities [10]. Piperazine derivatives have demonstrated significant biological activity; Piperazine structures have been successfully used as anti-cancer and anti-tumor drugs. In this work, a quantitative structure-activity relationship (QSAR) and in silico pharmacokinetics studies were performed on a series of piperazine derivatives with the aim of discovering more efficient mTORC1 inhibitors.

2. Material and Methods

QSAR study was conducted with the dataset available, including 129 piperazine derivatives, reported to inhibit mTORC1 by Kang, S.A. et al. [10]. This work selected 37 compounds based on such a criterion so that the present work deals with the most potent inhibitors. The selected compounds had to show high inhibitory activity with a minimum of $pIC_{50} > 5$ to consider only those showing the most intense action. Moreover, structural consistency was maintained by choosing compounds that possess the same core of the piperazine skeleton so that homogeneity within the data set would be ensured. Finally, in order to optimize computational resources because of the high intensity of DFT calculations, only representative compounds that showed a lot of promise were further pursued. Derivatives were constructed using ChemDraw Professional V. 16.0. Figure 2 represents the basic skeleton of the studied structures.

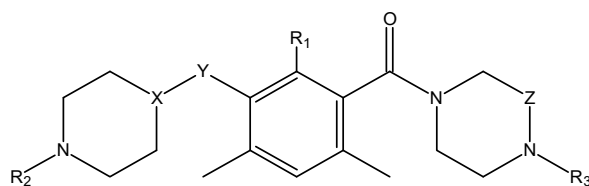


Figure 2. The basic skeleton of piperazine derivatives.

2.1. Calculation of Molecular Descriptors

The data set of investigated compounds was created by calculating the molecular descriptors of each molecule with ACD/ChemSketch 2016 and ChemOffice Professional V. 16.0 softwares. Furthermore, the density functional theory (DFT) method was used to determine their electronic descriptors by employing Becke's three-parameter hybrid function (B3LYP) with a basis set 6-31G+(d, p), which is available with Gaussian 09 software. Other quantum descriptors, such as the energy gap (E_{gap}), hardness (η), electronegativity (χ), and electrophilicity index (ω), were added and calculated using the following formulas [9–11]:

$$E_{\text{gap}} = E_{\text{LUMO}} - E_{\text{HOMO}}; \eta = (E_{\text{LUMO}} - E_{\text{HOMO}})/2; \chi = -(E_{\text{LUMO}} + E_{\text{HOMO}})/2; \omega = \chi^2/2\eta$$

With E_{HOMO} is the Highest occupied molecular orbital energy, E_{LUMO} is the Lowest unoccupied molecular orbital energy (E_{LUMO}).

2.2. Multiple Linear Regression (MLR)

Multiple linear regression (MLR) is one of the most basic and common modeling methods for QSAR studies used to date. MLR is preferred for its simplicity and ease of interpretation because the model assumes a linear relationship between the compound property Y , and its feature vector, denoted X , which is usually the molecular descriptors [10]. Thus, with the notion of X , the fitted model can predict the property of an unknown compound. MLR is vulnerable to descriptors that are correlated with each other, making it unable to decide which correlated sets may be more meaningful for the model [12].

The following equation represents a general expression for an RLM model:

$$Y = a_0 + a_1 X_1 + a_2 X_2 + a_3 X_3 + \dots + a_n X_n$$

In the above expression, Y is the response or dependent variable, X_1, X_2, \dots, X_n are descriptors (characteristics or independent variables) present in the model with corresponding regression coefficients a_1, a_2, \dots, a_n , respectively, and a_0 is the constant term of the model. The descriptors present in an MLR model should not be much intercorrelated. An MLR model that fits the data well will lead to a scatterplot (observed vs. calculated) showing a minimum deviation of the points from the fit line. The quality of an MLR model is determined from a number of measures described below.

2.3. Multiple Non-Linear Regression (MNLr)

The MNLr technique is a nonlinear (exponential, logarithmic, polynomial, etc.) approach to develop the mathematical model that best expresses the nonlinear variability of a molecular property or biological activity (Y) with respect to the molecular descriptors (X_i) [12,13]. In this case, we apply the MNLr approach to generate the QSAR model using the second-order polynomial model, which is based on the MLR model descriptors. The following equation is used to calculate the nonlinear connection between the molecular descriptors and the biological activity.

$$Y = a_0 + a_1 X_1 + b_1 X_1^2 + a_2 X_2 + b_2 X_2^2 \dots + a_n X_n + b_n X_n^2$$

where Y is the dependent variable (biological activity to be predicted), X_n are the independent variables (molecular descriptors), a_0 is the model constant, and a_n and b_n are the descriptor coefficients in the model equation.

2.4. Drug-Likeness Properties

We perform drug-like scoring of molecules that exhibit the highest potential biological activity (observed and predicted) in the inhibition of mTORC1. This is due to the importance of this procedure to identify the favorable structural properties for oral bioavailability of candidate drugs [14,15]. These predictions were developed based on the Lipinski's, Veber's and Egan's rules [16]. The drug-like profiles of the candidate molecules were predicted by the SwissADME webserver [17].

3. Results and Discussion

In this work, we used the XLSTAT 2016.3 software to perform the PCA analysis, the MLR and MNLr regressions [18,19]. Only 26 descriptors are retained, and they are introduced after the PCA principal component analysis. The MLR approach was used to create the QSAR models using 26 descriptors as inputs.

3.1. Multiple Linear Regression

Relationships with the pIC_{50} inhibitory activity indicator variable will be developed; multiple linear regression is used [20]. The best model obtained by this method is a linear combination of six molecular descriptors, namely energy E_{LUMO} , electrophilic index (ω), molar refractivity (MR), aqueous solubility (Log S), topological polar surface (PSA), and refractive index (n).

Each of the descriptors has an important role in the interaction of the piperazine derivatives with the target mTORC1. E_{LUMO} has the capability to accept electrons is one of the key properties characterizing the ability of a molecule to interact with the target protein, (ω) shows the ability of a molecule to act as an electrophile, hence to give or share electron pairs with nucleophilic sites on mTORC1, while (MR) accounts for the volume occupied by electrons, interacting in any molecule and allowing it to fit into the binding pocket of mTORC1, (Log S) affects the bioavailability and distribution of the inhibitor within the biological system and (PSA) is related to cell permeability by passive diffusion and interaction with the active site of mTORC1, lastly (n) is directly related to the polarizability of the molecule that is important, by itself, for noncovalent interactions crucial for effective inhibition.

The following equation provides the QSAR model obtained using the MLR approach:

$$pIC_{50} = 32.815 + 19.421E_{LUMO} + 10.521\omega + 1.428 MR + 1.214 \text{ Log S} - 3.95.10^{-2} PSA - 22.888 n$$

With: $N = 30$; $R = 0.86$; $R^2 = 0.74$; $R^2_{Adjusted} = 0.67$; $R^2_{test} = 0.54$; $MSE = 0.142$; $MSE = 0.377$;

$$Pr < 0.0001; F = 11.133; R^2_{CV} = 0.56$$

It appears from the equation that the six descriptors chosen are linearly related to the levels of inhibitory activity (pIC_{50}). The equation's given QSAR model is statistically credible, as shown by the higher coefficient of determination ($R^2 = 0.74$), mean squared error ($MSE = 0.142$) and the high degree of statistical confidence ($F = 11.133$). Also, the statistical significance of the QSAR model equation at a level higher than 95% is demonstrated by a p -value of less than 0.05 ($Pr < 0.0001$) in the equation.

Additionally, the internal validation correlation coefficient's value ($R^2_{CV} = 0.542$), which is higher than 0.5, demonstrates the MLR technique's QSAR model's high accuracy. When any element from the training set is removed, the model is poor when the value of R^2_{CV} is less than 0.6 and less than that of R^2 . The graphical depiction of the observed activity values and the anticipated values is shown in Figure 3 (pIC_{50}). The MLR model is used to determine the latter for the molecules in the test and training sets.

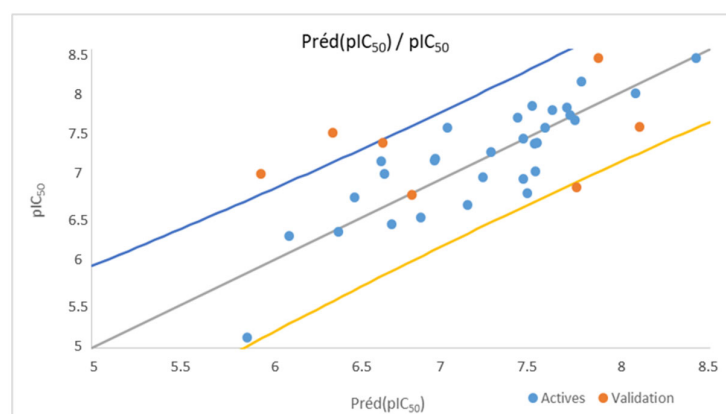


Figure 3. Correlation between observed activity values and predicted activity values via the MLR model.

Due to the low MSE value obtained, we can see from Figure 3 that there is a significant correlation between the distribution of observed and predicted pIC_{50} values. Therefore, it is evident that there is a correlation between the empirically determined values and those anticipated by the MLR model. It follows that the six MLR model descriptors have a strong linear association with the biological activity of pIC_{50} , which inhibits the activity of the cancer-causing protein mTORC1.

A novel nonlinear model is constructed utilizing the MNLR to optimize the correlation between the predicted activities acquired by the QSAR model developed via the MLR technique and the six molecular descriptors [21,22]. The following descriptors: E_{LUMO} , electrophilic index (ω), Molecular refractivity, aqueous solubility (Log S), topological polar surface area (PSA) and refractive index (n) are used as input parameters in these two techniques.

3.2. Multiple Nonlinear Regression

The resulting QSAR model via the MNLR technique is given by the following equation:

$$pIC_{50} = 724.114 + 45.307 E_{LUMO} + 22.195 \omega - 5.736 MR - 0.494 \text{Log S} - 0.023 \text{PSA} \\ - 798.318 n + 8.55 (E_{LUMO}^2) - 1.940 (\omega^2) + 0.222 (MR^2) - 0.106 (\text{Log S}^2) - \\ 9.10^{-6} (\text{PSA}^2) + 235.124 (n^2)$$

With: $N = 30$; $R = 0.88$; $R^2 = 0.78$; $R^2_{test} = 0.57$; $MSE = 0.163$; $RMSE = 0.404$; $R^2_{CV} = 0.53$

The obtained MNLR model had an excellent statistical performance: $R^2 = 0.78$, showing that the model fitted well with the training set. The cross-validation coefficient- $R^2_{CV} = 0.53$ -and external validation- $R^2_{test} = 0.57$ -produce evidence that the model is still predictive for unseen compounds, though with a moderate drop compared to the training set. This is within acceptable limits for QSAR models, particularly on complex biological

activities. We realize that the difference between R^2 and R^2_{CV} for the same model may indicate overfitting. Still, our central goal had been to relate the molecular descriptors linearly with the inhibitory activity. Whereas the MNLR model involved higher-order polynomial terms, the development of such had been intended to capture a fine nonlinear relationship among the independent variables without digressing from those basic linear associations established in the MLR model previously. Furthermore, the close match of the MLR and MNLR-predicted pIC_{50} values underlines the coherence of linearity in both of the modeling approaches. In addition, detailed validation methodologies have been carried out, including Y-randomization and applicability domain calculations, to ensure the models do not become an outcome of any dataset artifacts but instead genuine structure-activity relationships. With this modest difference between R^2 and R^2_{CV} , we still believe that the MNLR model is robust and generalizable enough to predict the inhibitory activity of any novel piperazine derivatives against mTORC1, we can see from Figure 4 the correlation between the distribution of observed and predicted pIC_{50} values. Internal and external validation is undertaken to ensure the fidelity of the predictive power of the developed QSAR models [23–28].

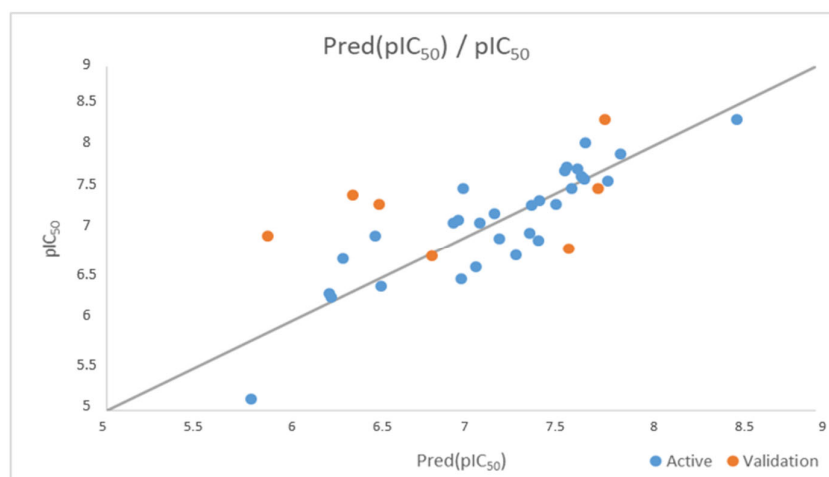


Figure 4. Correlation between observed activity values and predicted activity values via the MNLR model.

The external validation coefficient of determination (R^2_{test}), which is necessary to estimate the predictive power of the QSAR models to predict the inhibitory activity of other molecules that were not involved in the development of these models. Values R^2_{test} of 0.54 and 0.57 were obtained for the models MLR and MNLR, respectively. Values R^2_{test} of the both models are very similar, and all are greater than 0.5. Therefore, external validation of QSAR models confirms that these models have acceptable predictive potential.

The results of the internal and external validation of the QSAR models developed in this work are summarized in Table 1.

Table 1. Comparison of MLR and MNLR validation parameters.

Coefficients	R^2	R^2_{test}	MSE	RMSE
MLR	0.74	0.54	0.142	0.377
MNLR	0.78	0.57	0.163	0.404

When the coefficients (R , R^2 , MSE) of the MLR and MNLR models are compared, it is clear that the two proposed models are statistically significant and have good internal and external predictive ability. Accordingly, MLR and MNLR models exhibit a relationship between molecular descriptors (E_{LUMO} energy, electrophilicity index (ω), molar refractivity (MR), aqueous solubility (Log S), topological polar surface (PSA), and refraction (n)) and

the inhibitory activity of the mTORC1 protein (pIC_{50}). Subsequently, these QSAR models can be used to predict the activity values of additional compounds that can be engineered by piperazine substitution to produce new molecules with better activities than previously observed. Rather than developing new compounds and estimating their activities, we use a series of piperazine derivatives to find the best molecules to inhibit the mTORC1 protein. We chose these candidates based on the high activity values predicted by the QSAR models. Before choosing compounds with the greatest predicted biological activity, we perform two critical experiments to ensure that the predicted pIC_{50} values are accurate [23]. Y-randomization and applicability domain tests were performed. These two tests are used to eliminate the possibility of selecting one or more molecules whose activities were incorrectly predicted in this study [24,25]. We use a series of piperazine derivatives to find the best molecules to inhibit the mTORC1 protein. We chose these candidates based on the high activity values predicted by the QSAR models [26]. Before choosing compounds with the greatest predicted biological activity, we perform two critical experiments to ensure that the predicted pIC_{50} values are accurate. Y-randomization and applicability domain tests were performed. These two tests are used to eliminate the possibility of selecting one or more molecules whose activities were incorrectly predicted in this study. We use a series of piperazine derivatives to find the best molecules to inhibit the mTORC1 protein. We chose these candidates based on the high activity values predicted by the QSAR models.

Internal validation of both produced QSAR models has been effective. We execute an external validation to evaluate the precision and predictive strength of the developed QSAR models. The outcomes of the test are presented in the paragraph that follows.

3.3. Y-Randomization Test

Y-randomization test is performed on the original QSAR model created by the MLR approach to ensure the quality of the model. This test is used to eliminate the possibility of randomly finding a high association between the six molecular descriptors and mTORC1 inhibitory activity [27,28]. The Y-randomization test is carried out by distributing the Y values (pIC_{50}) 100 times at random without modifying the six descriptors. The development of the new QSAR models was made possible thanks to the random distribution of the pIC_{50} values to the six descriptors. Each new model has its own set of parameters (R, R^2 and Q^2). The values of R, R^2 and Q^2 acquired by the randomly created models are lower than the values produced by the original model. These results confirm the validity of the MLR model and show that the relationship between the six descriptors and biological activity is not a coincidence. Therefore, we can be sure that the pIC_{50} predicted by the MLR models based on the six descriptors of the original model are not random (Table 2).

Table 2. Résultats du test de randomisation en Y.

Model	R	R^2	Q^2	Model	R	R^2	Q^2
Original	0.862	0.744	0.561	Random 51	0.449	0.202	-0.371
Random 1	0.249	0.062	-0.497	Random 52	0.560	0.314	-0.207
Random 2	0.536	0.287	-0.076	Random 53	0.546	0.298	-0.305
Random 3	0.636	0.404	-0.065	Random 54	0.488	0.238	-0.313
Random 4	0.339	0.115	-0.406	Random 55	0.434	0.189	-0.411
Random 5	0.373	0.139	-0.568	Random 56	0.158	0.025	-0.574
Random 6	0.429	0.184	-0.458	Random 57	0.251	0.063	-0.688
Random 7	0.286	0.082	-1.218	Random 58	0.426	0.182	-0.388
Random 8	0.415	0.172	-0.514	Random 59	0.233	0.054	-0.538
Random 9	0.590	0.348	-0.096	Random 60	0.588	0.346	-0.171
Random 10	0.463	0.215	-0.534	Random 61	0.464	0.215	-0.450
Random 11	0.605	0.366	-0.054	Random 62	0.420	0.177	-0.381
Random 12	0.355	0.126	-0.465	Random 63	0.627	0.393	0.012
Random 13	0.391	0.153	-0.420				

Table 2. Cont.

Model	R	R ²	Q ²	Model	R	R ²	Q ²
Random 14	0.272	0.074	−0.596	Random 64	0.541	0.293	−0.327
Random 15	0.370	0.137	−0.603	Random 65	0.528	0.279	−0.136
Random 16	0.428	0.183	−0.480	Random 66	0.459	0.210	−0.360
Random 17	0.484	0.234	−0.235	Random 67	0.480	0.231	−0.424
Random 18	0.407	0.166	−0.411	Random 68	0.409	0.168	−0.383
Random 19	0.707	0.500	0.067	Random 69	0.407	0.166	−0.435
Random 20	0.289	0.084	−0.594	Random 70	0.388	0.150	−0.521
Random 21	0.641	0.411	0.050	Random 71	0.427	0.182	−0.481
Random 22	0.663	0.440	0.044	Random 72	0.392	0.154	−0.402
Random 23	0.630	0.397	−0.064	Random 73	0.559	0.312	−0.024
Random 24	0.435	0.190	−0.235	Random 74	0.543	0.295	−0.225
Random 25	0.487	0.238	−0.295	Random 75	0.357	0.127	−0.429
Random 26	0.497	0.247	−0.312	Random 76	0.604	0.364	−0.293
Random 27	0.352	0.124	−0.442	Random 77	0.497	0.247	−0.437
Random 28	0.693	0.480	0.201	Random 78	0.408	0.167	−0.463
Random 29	0.577	0.333	−0.248	Random 79	0.294	0.086	−0.676
Random 30	0.451	0.203	−0.221	Random 80	0.551	0.303	−0.224
Random 31	0.304	0.092	−0.588	Random 81	0.422	0.178	−0.439
Random 32	0.446	0.199	−0.579	Random 82	0.447	0.200	−0.287
Random 33	0.301	0.091	−0.521	Random 83	0.427	0.182	−0.470
Random 34	0.586	0.344	−0.217	Random 84	0.334	0.111	−0.410
Random 35	0.428	0.184	−0.495	Random 85	0.554	0.306	−0.169
Random 36	0.420	0.176	−0.358	Random 86	0.528	0.279	−0.263
Random 37	0.525	0.276	−0.446	Random 87	0.583	0.340	−0.103
Random 38	0.553	0.306	−0.191	Random 88	0.487	0.237	−0.344
Random 39	0.326	0.106	−0.431	Random 89	0.525	0.276	−0.280
Random 40	0.499	0.249	−0.206	Random 90	0.550	0.302	−0.190
Random 41	0.588	0.346	−0.159	Random 91	0.318	0.101	−0.645
Random 42	0.337	0.113	−0.747	Random 92	0.364	0.133	−0.420
Random 43	0.518	0.268	−0.178	Random 93	0.462	0.213	−0.407
Random 44	0.322	0.104	−0.478	Random 94	0.478	0.228	−0.177
Random 45	0.430	0.185	−0.527	Random 95	0.474	0.224	−0.347
Random 46	0.466	0.217	−0.286	Random 96	0.497	0.247	−0.257
Random 47	0.643	0.414	−0.041	Random 97	0.206	0.042	−0.622
Random 48	0.494	0.244	−0.184	Random 98	0.385	0.148	−0.522
Random 49	0.353	0.125	−0.567	Random 99	0.306	0.093	−0.508
Random 50	0.470	0.221	−0.291	Random 100	0.332	0.110	−0.393

3.4. Applicability Domain

The applicability domain was checked, in accordance with literature [29], by a Williams plot representing the distribution of the normalized residuals as a function of the leverage values of the compounds of the dataset. Figure 5 refers to the Williams plot indicating that all compounds fall within the applicability domain defined by this model, for which the critical leverage threshold h^* was set to 0.58 and the limits of residuals were set at ± 2.5 . This confirms that none of the compounds are outliers or undue leverage to the model and hence the predictions would be valid. This data set indeed represents a diverse library of piperazine derivatives spanning a wide chemical space relevant to the inhibition of mTORC1. In contrast, all the well-known mTORC1 inhibitors have larger, more complex structures compared with Everolimus, Temsirolimus, and Ridaforolimus; the selected compounds represent simpler yet potent derivatives. The performed AD analysis confirmed that these molecules fall well within the reliable predictive scope of the model.

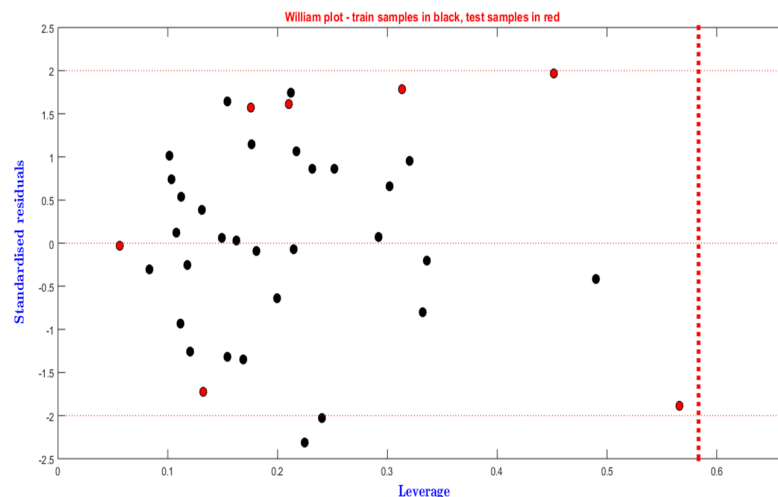


Figure 5. William's plot of leverage-normalized residuals for the MLR pIC_{50} model (with $h^* = 0.58$ and residual limits $y = \pm 2.5$).

3.5. Identification of Candidate Inhibitors

The close match of the MLR and MNLR-predicted pIC_{50} values underlines the coherence of linearity in both of the modeling approaches. We chose seven compounds with high pIC_{50} values predicted by the MLR model (Table 3) [30,31]. Compared to the drugs Everolimus, Temsirolimus and Ridaforolimus, these seven compounds all have higher predicted pIC_{50} values.

Table 3. Values predicted by developed QSAR models and experimental pIC_{50} values for Everolimus, Temsirolimus, and Ridaforolimus.

Compound No.	Pred (pIC_{50}) mTORC1	
	MLR	MNLR
2	8.421	8.5574
29	8.101	7.7738
13	8.078	7.8999
4	7.869	7.813
10	7.77	7.7024
71	7.743	7.6084
25	7.736	7.8294
	pIC_{50} exp.	
Everolimus	8.26	
Temsirolimus	5.8	
Ridaforolimus	9.7	

The pIC_{50} values estimated from both the MLR and MNLR models have reasonable predictions, as seen in Table 3. This agreement looks promising and therefore underlines the robustness of our QSAR strategy in identifying potent inhibitors targeting mTORC1. It is tough to highlight a single best compound, as its pIC_{50} values all share similar prediction views. In this regard, an in-silico ADME analysis was conducted for the seven high- pIC_{50} compounds to further investigate their overall drug-likeness properties.

3.6. Evaluation of Drug-Likeness Properties

Table 4 summarizes the calculated ADME profiles, indicating that five compounds (2, 4, 13, 25, and 71) possess excellent pharmacokinetic properties with high absorption profiles and complying with the major drug-likeness rules. These parameters provided the rationale for identifying the five candidates as the most promising ones for further development.

Table 4. The in silico ADME results of the seven proposed compounds.

Property	Absp	MW	LogP	NHD	NHA	NROT	TPSA (Å ²)	SA
Rule	-	<500	<5	<5	<10	<10	<140	0 < SA < 10
2	High	627.77	2.27	2	8	9	109.71	5.85
29	Weak	627.77	2.59	2	7	9	106.70	4.45
13	High	573.68	3.74	2	5	7	82.84	4.43
4	High	602.77	2.80	2	6	6	100.09	5.56
10	Weak	585.76	2.21	2	5	7	124.80	4.97
25	High	524.66	2.27	2	4	7	95.73	4.34
71	High	608.70	2.21	1	8	7	122.36	4.21
Everolimus	Weak	958.22	6.58	3	14	9	204.66	10
Temsirolimus	Weak	1030.2	6.82	4	16	11	241.96	10
Ridaforolimus	Weak	990.21	7.10	2	14	8	211.31	10
Property		Lipinski's Violation		Muegge's Violation		Veber's Violation		Egan's Violation
Rule		≤2		≤1		≤1		≤1
2		1		0		0		0
29		1		0		0		0
13		1		0		0		0
4		1		0		0		0
10		1		0		0		0
25		1		0		0		0
71		1		0		0		0
Everolimus		2		4		1		1
Temsirolimus		2		4		2		2
Ridaforolimus		2		4		1		1

Absp: absorption; MW: Molecular weight; LogP: Lipophilicity; NHA: Number of hydrogen bond acceptors; NHD: Number of donor hydrogen bonds; NROT: Number of rotatable links; TPSA: Topological polar surface; SA: Synthetic Accessibility.

The main objective of this study was to predict the drug-likeness of the seven selected piperazine derivatives (2, 4, 10, 13, 25, 29, and 71) by evaluating their pharmacokinetic profiles using the SwissADME platform [16]. The in silico ADME analysis (Table 4) showed that five compounds (2, 4, 13, 25, and 71) exhibit high absorption potential and adhere to key drug-likeness criteria (Lipinski, Veber, Meugee, and Egan rules), suggesting good oral bioavailability, we've showcased the 3D structures of selected molecules in Figure 6. In comparison, the marketed drugs Everolimus, Temsirolimus, and Ridaforolimus show multiple violations of these rules, indicating potentially lower bioavailability. Additionally, the synthetic accessibility (SA) scores for the proposed compounds (ranging from 4.2 to 5.56) suggest they are simpler to synthesize compared to the more complex marketed drugs (SA = 10). All the five selected compounds had a TPSA lower than 140 Å² and less than 10 NROT, which enhanced their molecular flexibility to have better interaction with the mTORC1 receptor at low energy. This, in turn, contributed to the better cell permeability and favorable pharmacokinetic profiles. Finally, the synthetic accessibility scores of the compounds were below that of the marketed drugs; this demonstrates easy and cheap syntheses. Taken together, these properties imply the selected piperazine derivatives have increased absorption but perhaps of more importance, the potential for reduced side effects and improved pharmacokinetics compared to the existing mTORC1 inhibitors.

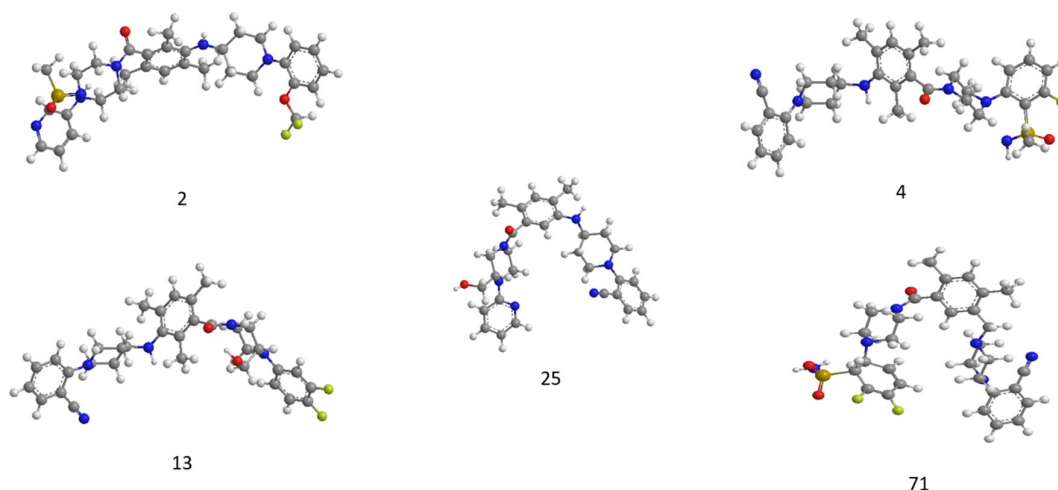


Figure 6. 3D structures of selected molecules (2, 4, 13, 25, and 71) by evaluating pharmacokinetic properties ADME.

4. Conclusions

The experimental study combined DFT, QSAR modeling, and in silico ADME analyses in investigating a series of thirty-seven piperazine derivatives as potential inhibitors of mTORC1 for cancer therapy. All molecular descriptors calculated in the present study were electronic, topological, geometrical, and physicochemical parameters computed using Gaussian 09 and ChemsSketch and ChemOffice software. The PCA, MLR, and MNLR were employed to develop robust QSAR models. MLR and MNLR models showed good predictive power with R^2 of 0.74 and 0.78, respectively, and with R^2CV of 0.56 and 0.53, respectively. These models pinpointed six important molecular descriptors—ELUMO, electrophilicity index (ω), MR, Log S, PSA, and refractive index (n)—whose values strongly correlate with the inhibitory activity, expressed as pIC_{50} , against mTORC1. By using these QSAR models along with in silico pharmacokinetic profiling, we identified five compounds, 2, 4, 13, 25, and 71, to be the most promising mTORC1 inhibitors. These few selected compounds, in addition to having better predicted pIC_{50} than known drugs like Everolimus, Temsirolimus, and Ridaforolimus, showed favorable pharmacokinetic properties. More precisely, they exhibit high absorption potential and follow all the drug-likeness rules of Lipinski, Muegge, Veber, and Egan's thus suggesting good oral bioavailability with less probability for adverse effects. The low scores obtained for synthetic accessibility indicate that these compounds are easier and less expensive to synthesize compared to the more complex, advertised drugs. These results enable consideration of the identified piperazine derivatives as effective and safer alternatives to current mTORC1 inhibitors. Therefore, the predicted inhibitory activity and pharmacokinetic profile of such compounds need to be experimentally validated by in vitro and in vivo studies. Thus, future research should be directed toward synthesizing such candidates and elucidating their biological efficacy and safety to facilitate further progression toward clinical development.

Author Contributions: Conceptualization: E.M.K., O.A., F.S., H.N. and O.D.; methodology: S.C.; software: S.C.; validation: A.E., S.E.K. and S.C.; formal analysis: E.M.K.; investigation: E.M.K. and S.C.; resources: S.C.; data curation: E.M.K.; writing—original draft preparation: E.M.K. and F.S.; writing—review and editing: E.M.K. and M.E.K.; visualization: A.E., S.E.K., M.T. and S.C.; supervision: S.C.; project administration: S.C.; funding acquisition: S.E.K. All authors have read and agreed to the published version of the manuscript.

Funding: This research received no external funding.

Data Availability Statement: Not applicable.

Conflicts of Interest: The authors declare no conflict of interest.

References

1. Stueven, N.A.; Schlaeger, N.M.; Monte, A.P.; Hwang, S.-P.L.; Huang, C.-c. A novel stilbene-like compound that inhibits melanoma growth by regulating melanocyte differentiation and proliferation. *Toxicol. Appl. Pharmacol.* **2017**, *337*, 30–38. [[CrossRef](#)] [[PubMed](#)]
2. Marra, A.; Ferrone, C.R.; Fuscillo, C.; Scognamiglio, G.; Ferrone, S.; Pepe, S.; Perri, F.; Sabbatino, F. Translational research in cutaneous melanoma: New therapeutic perspectives. *Anti. Canc. Agents Med. Chem.* **2018**, *18*, 166–181. [[CrossRef](#)] [[PubMed](#)]
3. Mioc, M.; Pavel, I.Z.; Ghiulai, R.; Coricovac, D.E.; Farcaş, C.; Mihali, C.-V.; Oprean, C.; Serafim, V.; Popovici, R.A.; Dehelean, C.A. The cytotoxic effects of betulin-conjugated gold nanoparticles as stable formulations in normal and melanoma cells. *Front. Pharmacol.* **2018**, *9*, 429. [[CrossRef](#)] [[PubMed](#)]
4. Theodosakis, N.; Micevic, G.; Langdon, C.G.; Ventura, A.; Means, R.; Stern, D.F.; Bosenberg, M.W. p90RSK blockade inhibits dual BRAF and MEK inhibitor-resistant melanoma by targeting protein synthesis. *J. Invest. Dermatol.* **2017**, *137*, 2187–2196. [[CrossRef](#)] [[PubMed](#)]
5. Faes, S.; Demartines, N.; Dormond, O. Resistance to mTORC1 inhibitors in cancer therapy: From kinase mutations to intratumoral heterogeneity of kinase activity. *Oxidative Med. Cell. Longev.* **2017**, *2017*, 1726078. [[CrossRef](#)]
6. Brito, A.F.; Moreira, L.K.; Menegatti, R.; Costa, E.A. Piperazine derivatives with central pharmacological activity used as therapeutic tools. *Fundam. Clin. Pharmacol.* **2019**, *33*, 13–24. [[CrossRef](#)]
7. Ganesan, A. The impact of natural products upon modern drug discovery. *Curr. Opin. Chem. Biol.* **2008**, *12*, 306–317. [[CrossRef](#)]
8. Chaube, U.J.; Rawal, R.; Jha, A.B.; Variya, B.; Bhatt, H.G. Design and development of Tetrahydro-Quinoline derivatives as dual mTOR-C1/C2 inhibitors for the treatment of lung cancer. *Bioorganic Chem.* **2021**, *106*, 104501. [[CrossRef](#)]
9. Kaavin, K.; Naresh, D.; Yogeshkumar, M.R.; Prakash, M.K.; Janarthanan, S.; Krishnan, M.M.; Malathi, M. In-silico DFT studies and molecular docking evaluation of benzimidazo methoxy quinoline-2-one ligand and its Co, Ni, Cu and Zn complexes as potential inhibitors of Bcl-2, Caspase-3, EGFR, mTOR, and PI3K, cancer-causing proteins. *Chem. Phys. Impact* **2024**, *8*, 100418. [[CrossRef](#)]
10. Kang, S.A.; O'Neill, D.J.; Machl, A.W.; Lumpkin, C.J.; Galda, S.N.; Sengupta, S.; Saiah, E. Discovery of small-molecule selective mTORC1 inhibitors via direct inhibition of glucose transporters. *Cell Chem. Biol.* **2019**, *26*, 1203–1213. [[CrossRef](#)]
11. Hong, H.; Xie, Q.; Ge, W.; Qian, F.; Fang, H.; Shi, L.; Tong, W. Mold2, molecular descriptors from 2D structures for chemoinformatics and toxicoinformatics. *J. Chem. Inf. Model.* **2008**, *48*, 1337–1344. [[CrossRef](#)] [[PubMed](#)]
12. Consonni, V.; Todeschini, R. Molecular descriptors. In *Recent Advances in QSAR Studies*; Springer: Dordrecht, The Netherlands, 2010; pp. 29–102. [[CrossRef](#)]
13. Gozalbes, R.; Doucet, J.P.; Derouin, F. Application of topological descriptors in QSAR and drug design: History and new trends. *Curr. Drug Targets-Infect. Disord.* **2002**, *2*, 93–102. [[CrossRef](#)] [[PubMed](#)]
14. Chtita, S.; Hmamouchi, R.; Larif, M.; Ghamali, M.; Bouachrine, M.; Lakhli, T. QSPR studies of 9-anilinoacridine derivatives for their DNA drug binding properties based on density functional theory using statistical methods: Model, validation and influencing factors. *J. Taibah Univ. Sci.* **2016**, *10*, 868–876. [[CrossRef](#)]
15. Usta, O.; McCarty, W.; Bale, S.; Hegde, M.; Jindal, R.; Bhushan, A.; Golberg, I.; Yarmush, M. Microengineered cell and tissue systems for drug screening and toxicology applications: Evolution of in-vitro liver technologies. *Technology* **2015**, *3*, 1–26. [[CrossRef](#)] [[PubMed](#)]
16. Saqib, U.; Kumar, B.; Siddiqi, M.I. Structural investigations of anthranilimide derivatives by CoMFA and CoMSIA 3D-QSAR studies reveal novel insight into their structures toward glycogen phosphorylase inhibition. *SAR QSAR Environ. Res.* **2011**, *22*, 411–449. [[CrossRef](#)]
17. Dahmani, R.; Manachou, M.; Belaidi, S.; Chtita, S.; Boughdiri, S. Structural characterization and QSAR modeling of 1,2,4-triazole derivatives as α -glucosidase inhibitors. *New J. Chem.* **2021**, *45*, 1253–1261. [[CrossRef](#)]
18. Karelson, M.; Lobanov, V.S.; Katritzky, A.R. Quantum-chemical descriptors in QSAR/QSPR studies. *Chem. Rev.* **1996**, *96*, 1027–1044. [[CrossRef](#)]
19. Fouedjou, R.T.; Chtita, S.; Bakhouch, M.; Belaidi, S.; Ouassaf, M.; Djoumbissie, L.A.; Abul Qais, F. Cameroonian medicinal plants as potential candidates of SARS-CoV-2 inhibitors. *J. Biomol. Struct. Dyn.* **2021**, *40*, 8615–8629. [[CrossRef](#)]
20. Katritzky, A.R.; Gordeeva, E.V. Traditional topological indexes vs. electronic, geometrical, and combined molecular descriptors in QSAR/QSPR research. *J. Chem. Inf. Comput. Sci.* **1993**, *33*, 835–857. [[CrossRef](#)]
21. Emmert-Streib, F. *Statistical Modelling of Molecular Descriptors in QSAR/QSPR*; John Wiley & Sons: Hoboken, NJ, USA, 2012. [[CrossRef](#)]
22. Chtita, S.; Belhassan, A.; Bakhouch, M.; Taourati, A.I.; Aouidate, A.; Belaidi, S.; Lakhli, T. QSAR study of unsymmetrical aromatic disulfides as potent avian SARS-CoV main protease inhibitors using quantum chemical descriptors and statistical methods. *Chemom. Intell. Lab. Syst.* **2021**, *210*, 104266. [[CrossRef](#)]
23. Aouidate, A.; Ghaleb, A.; Ghamali, M.; Chtita, S.; Sbai, A.; Bouachrine, M.; Lakhli, T. Combined 3D-QSAR and molecular docking study on 7, 8-dialkyl-1, 3-diaminopyrrolo-[3, 2-f] Quinazoline series compounds to understand the binding mechanism of DHFR inhibitors. *J. Mol. Struct.* **2017**, *1139*, 319–327. [[CrossRef](#)]
24. Hansch, C.; Kurup, A.; Garg, R.; Gao, H. Chem-bioinformatics and QSAR: A review of QSAR lacking positive hydrophobic terms. *Chem. Rev.* **2001**, *101*, 619–672. [[CrossRef](#)] [[PubMed](#)]
25. Ghamali, M.; Chtita, S.; Hmamouchi, R.; Adad, A.; Bouachrine, M.; Lakhli, T. The inhibitory activity of aldose reductase of flavonoid compounds: Combining DFT and QSAR calculations. *J. Taibah Univ. Sci.* **2016**, *10*, 534–542. [[CrossRef](#)]

26. Garg, R.; Gupta, S.P.; Gao, H.; Babu, M.S.; Debnath, A.K.; Hansch, C. Comparative quantitative structure—Activity relationship studies on anti-HIV drugs. *Chem. Rev.* **1999**, *99*, 3525–3602. [[CrossRef](#)]
27. Aouidate, A.; Ghaleb, A.; Ghamali, M.; Chtita, S.; Ousaa, A.; Sbai, A.; Lakhlifi, T. Furanone derivatives as new inhibitors of CDC7 kinase: Development of structure activity relationship model using 3D QSAR, molecular docking, and in silico ADMET. *Struct. Chem.* **2018**, *29*, 1031–1043. [[CrossRef](#)]
28. Kumari, C.; Abulaish, M.; Subbarao, N. Exploring molecular descriptors and fingerprints to predict mTOR kinase inhibitors using machine learning techniques. *IEEE/ACM Trans. Comput. Biol. Bioinform.* **2020**, *18*, 1902–1913. [[CrossRef](#)]
29. Daoui, O.; Elkhatabi, S.; Chtita, S.; Elkhalabi, R.; Zgou, H.; Benjelloun, A.T. QSAR, molecular docking and ADMET properties in silico studies of novel 4, 5, 6, 7-tetrahydrobenzo [D]-thiazol-2-Yl derivatives derived from dimedone as potent anti-tumor agents through inhibition of C-Met receptor tyrosine kinase. *Heliyon* **2021**, *7*, e07463. [[CrossRef](#)]
30. Chen, B.; Wild, D.J. PubChem BioAssays as a data source for predictive models. *J. Mol. Graph. Model.* **2010**, *28*, 420–426. [[CrossRef](#)]
31. Chtita, S.; Aouidate, A.; Belhassan, A.; Ousaa, A.; Taourati, A.I.; Elidrissi, B.; Lakhlifi, T. QSAR study of N-substituted oseltamivir derivatives as potent avian influenza virus H5N1 inhibitors using quantum chemical descriptors and statistical methods. *New J. Chem.* **2020**, *44*, 1747–1760. [[CrossRef](#)]

Disclaimer/Publisher’s Note: The statements, opinions and data contained in all publications are solely those of the individual author(s) and contributor(s) and not of MDPI and/or the editor(s). MDPI and/or the editor(s) disclaim responsibility for any injury to people or property resulting from any ideas, methods, instructions or products referred to in the content.